GEOPHYSICAL RESEARCH LETTERS, VOL. 34, L03401, doi:10.1029/2006GL028848, 2007

Dynamic coupling of volcanic CO_2 flow and wind at the Horseshoe Lake tree kill, Mammoth Mountain, California

J. L. Lewicki,[1] G. E. Hilley,[2] T. Tosha,[3] R. Aoyagi,[4] K. Yamamoto,[4] and S. M. Benson[1]

Received 28 November 2006; revised 21 December 2006; accepted 3 January 2007; published 1 February 2007.

[1] We investigate spatio-temporal relationships between soil CO_2 flux (F_{CO2}), meteorological variables, and topography over a ten-day period (09/12/2006 to 09/21/2006) at the Horseshoe Lake tree kill, Mammoth Mountain, CA. Total CO_2 discharge varied from 16 to 52 t d^{-1}, suggesting a decline in CO_2 emissions over decadal timescales. We observed systematic changes in F_{CO2} in space and time in association with a weather front with relatively high wind speeds from the west and low atmospheric pressures. The largest F_{CO2} changes were observed in relatively high elevation areas. The variations in F_{CO2} may be due to dynamic coupling of wind-driven airflow through the subsurface and flow of source CO_2 at depth. Our results highlight the influence of weather fronts on volcanic gas flow in the near-surface environment and how this influence can vary spatially within a study area. **Citation:** Lewicki, J. L., G. E. Hilley, T. Tosha, R. Aoyagi, K. Yamamoto, and S. M. Benson (2007), Dynamic coupling of volcanic CO_2 flow and wind at the Horseshoe Lake tree kill, Mammoth Mountain, California, *Geophys. Res. Lett.*, *34*, L03401, doi:10.1029/2006GL028848.

1. Introduction

[2] Spatial and temporal variations in soil CO_2 fluxes (F_{CO2}) have been measured in many volcanic and hydrothermal systems worldwide [e.g., *Farrar et al.*, 1995; *Koepenick et al.*, 1996; *Giammanco et al.*, 1997; *Chiodini et al.*, 1998; *Werner et al.*, 2000; *Bergfeld et al.*, 2001; *Salazar et al.*, 2001; *Gerlach et al.*, 2001; *Rogie et al.*, 2001; *Lewicki et al.*, 2003] and used as a tool for volcano and seismotectonic monitoring, geothermal exploration, delineation of fault and fracture zones, and estimation of the contribution of CO_2 from volcanic and hydrothermal sources to the global carbon cycle. Diffuse CO_2 emissions have been intensely studied at Mammoth Mountain, a dacitic volcano located on the southwestern rim of Long Valley caldera, eastern California. An eleven-month-long seismic swarm occurred at Mammoth Mountain in 1989, possibly related to dike intrusion and/or fluid migration [*Hill*, 1996; *Hill and Prejean*, 2005]. Tree kills then formed in several areas on Mammoth Mountain due to diffuse emissions of magmatic CO_2 resulting in high CO_2 concentrations in the root zone [e.g., *Farrar et al.*, 1995].

[3] The largest of these tree kills is located on the northwest shore of Horseshoe Lake, on the flank of Mammoth Mountain (hereafter referred to as the Horseshoe Lake tree kill, HLTK; Figure 1). Extensive monitoring of subsurface CO_2 concentrations and F_{CO2} has sometimes resulted in large differences (e.g., factor of 2–3) in the total CO_2 discharge measured by different researchers [*Gerlach et al.*, 1998; *Farrar et al.*, 1998]. Studies have also reported large diurnal to seasonal fluctuations in time series of soil CO_2 concentrations, F_{CO2}, and total CO_2 discharges that appear to be due to variations in meteorological and hydrologic processes [e.g., *McGee and Gerlach*, 1998; *McGee et al.*, 2000; *Rogie et al.*, 2001]. In particular, *Rogie et al.* [2001] continuously monitored F_{CO2} at a fixed location within the tree kill, and found correlations between F_{CO2}, wind speed, and atmospheric pressure, but these relationships varied depending on the frequency of fluctuation. Also, *McGee et al.* [2000] showed that diurnal changes in soil CO_2 concentrations were largely controlled by local orographic winds, and although poorly understood, were likely also influenced by relatively infrequent weather fronts with strong winds.

[4] These previous studies at the HLTK quantified the temporal response of CO_2 flow to meteorological parameters. However, it is still unclear if the F_{CO2} is only modulated by meteorological parameters as some simple models predict (e.g., barometric pumping), or if the F_{CO2} spatial distribution itself changes in response to local meteorological and topographic conditions. While measuring time series of the F_{CO2} spatial distribution would place important constraints on the nature of subsurface CO_2 flow and its response to atmospheric processes, acquisition of such a time series that captures high-frequency (i.e., semi-diurnal to diurnal) fluctuations would be difficult due to the labor-intensive nature of the measurements. However, measuring changes in the F_{CO2} spatial distribution associated with lower-frequency events such as passing weather fronts on a daily basis is possible.

[5] Here we report spatio-temporal variations in F_{CO2} at the HLTK, and investigate how they are related to meteorological variables and topography over a ten-day period during which a weather front, characterized by relatively high wind speeds and low atmospheric pressures, occurred. Unexpectedly, we observed a decrease in F_{CO2} associated with the weather front and the decline systematically propagated from relatively high (western) to low (eastern) elevation areas. Following cessation of elevated winds, F_{CO2} gradually returned to previous levels, first in the low (eastern) then the high (western) elevation regions. We propose potential linkages between wind, topography, and

[1]Earth Sciences Division, Lawrence Berkeley National Laboratory, Berkeley, California, USA.
[2]Department of Geological and Environmental Sciences, Stanford University, Stanford, California, USA.
[3]Institute of Geo-Resources and Environment, National Institute of Advanced Industrial Science and Technology, Tsukuba, Japan.
[4]Mizuho Information and Research Institute, Tokyo, Japan.

0094-8276/07/2006GL028848$05.00

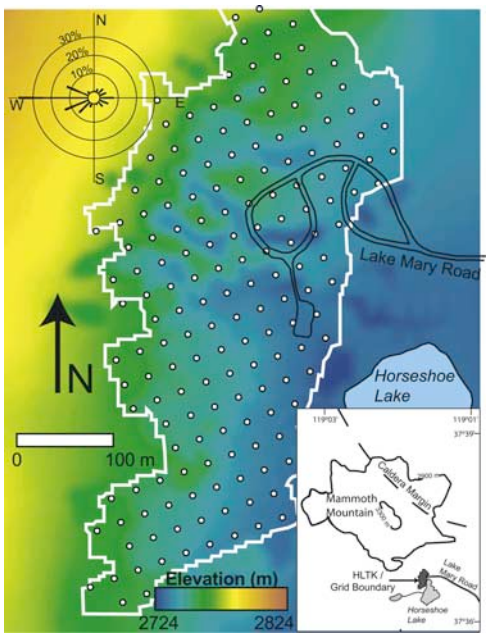

Figure 1. Digital elevation model of Horseshoe Lake tree kill (HLTK) area showing F_{CO2} survey grid points (white dots). Wind rose in upper left corner shows frequency of occurrence of wind directions over study period.

CO_2 flow at the HLTK, and discuss implications for future studies of volcanic and hydrothermal CO_2 emissions.

2. Methods

[6] Topography at the HLTK was surveyed using a Contour XLRic laser range finder (LaserCraft, Inc., Norcross, GA) with simultaneous measurements for bearing and azimuth. Precisions of range and angular measurements are 10 cm and 0.1°, respectively. Field surveyed data were merged with spot elevations provided by the National Elevation Dataset (NED) to create a digital elevation model of the study area (Figure 1).

[7] Wind speed and direction were measured at 2.5 m height at 10 Hz using a Gill WindMaster Pro three-axis sonic anemometer (Gill Instruments, Ltd, Lymington, United Kingdom) with resolutions of 0.01 m s^{-1} and 0.1°, respectively. Atmospheric pressure (±0.5 hPa) was measured using a Vaisala PTB101B barometer (Vaisala, Inc., Woburn, MA). Atmospheric temperature (±0.6°C) and relative humidity (±3%) were measured using a Vaisala HMP50 humidity and temperature probe. Soil moisture profiles (10 and 30 cm depth) were measured at two locations using ECH_2O (Decagon Devices, Pullman, WA) soil moisture probes with resolutions of 0.002 volume fraction. Soil temperature profiles (10, 20, and 30 cm depth) were measured at two locations with thermocouples. All meteorologic and soil parameters were measured from 09/10/2006 to 10/24/2006 and averaged over 30-minute intervals.

[8] F_{CO2} was measured using a WEST Systems Fluxmeter (WEST Systems, Pisa, Italy) based on the accumulation chamber method [*Chiodini et al.*, 1998], with accuracy and repeatability of −12.5% [*Evans et al.*, 2001] and ±10% [*Chiodini et al.*, 1998], respectively. F_{CO2} was measured at 170 grid points at 27-m spacing in the HLTK (Figure 1). F_{CO2} measurements were repeated in the same order along the grid each day from 09/12/2006 to 09/21/2006 between 07:00 and 15:00, with the exception of 09/15/2006 when no measurements were made. A stochastic simulation procedure based on a sequential Gaussian simulation (sGs) algorithm from GSLIB [*Deutsch and Journel*, 1998] was used to map F_{CO2} and estimate total CO_2 discharge from the study area [e.g., *Cardellini et al.*, 2003; *Lewicki et al.*, 2005]. One thousand simulations were conducted based on the measured grid data set for each day and used to produce a map of the F_{CO2} values expected at the grid cells (5 × 5 m) using a point-by-point average of the realizations. CO_2 discharge from the study area was calculated for each realization by multiplying the simulated F_{CO2} value for each grid cell by 25 m^2 and summing these products. The mean and 95% lower and upper bounds of the CO_2 discharges simulated for 1000 realizations are assumed to be the characteristic CO_2 discharge for the study area and its uncertainty, respectively.

3. Results

[9] No precipitation occurred at the HLTK from 09/09/2006 to 09/21/2006. Air temperatures ranged from −8.3 to 20.8°C. Winds were predominantly from the west (Figure 1). Measured F_{CO2} ranged from <1 to ~9600 g m^{-2} d^{-1} and total CO_2 discharges varied by a factor of ~3, from 16 to 52 t d^{-1} (Figures 2 and S1[1]). F_{CO2} was generally highest in the central portion of the area, and the spatial distribution remained relatively stable during the first two days (09/12/2006–09/13/2006) of observation (Figures 2a, 2b, and 3a). During this time, average daily wind speeds were ≤1.5 m s^{-1}, while average atmospheric pressure was >735 mbar. However, as a weather front passed through the region and average daily wind speed and pressure increased and decreased, respectively, to 3.5 m s^{-1} and <730 mbar (09/14/2006–09/15/2006), the area of relatively high F_{CO2} began to contract in size to the down-slope (east-central) region of the study area (Figures 2c and 3b). Contraction continued while wind speed dropped back to 1.5 m s^{-1} and pressure rebounded to 733 mbar on 09/16/2006 (Figures 2d and 3c). As wind speed and atmospheric pressure stabilized on 09/17/2006 to 09/18/2006, F_{CO2} recovered, with elevated fluxes migrating from the lower (eastern) to higher (western) elevation zones (Figures 2e, 2f, 3d, and 3e). Then, on 09/19/2006, wind speed rose and pressure declined, partially interrupting the F_{CO2} recovery (Figures 2g and 3f). From 09/19/2006 to 09/21/2006, while average daily wind speed declined and pressure remained constant, F_{CO2} continued to recover (Figures 2g, 2i, 3g, and 3h).

[10] CO_2 discharge showed the highest degree of positive correlation (correlation coefficient = 0.75) with average daily atmospheric pressure and negative correlation (correlation coefficient = −0.61) with average daily wind speed at one-day time lag (Figure S1). Average daily wind speed and atmospheric pressure were strongly negatively correlated (correlation coefficient = −0.76 to −0.87) at zero

[1] Auxiliary materials are available in the HTML. doi:10.1029/2006GL028848.

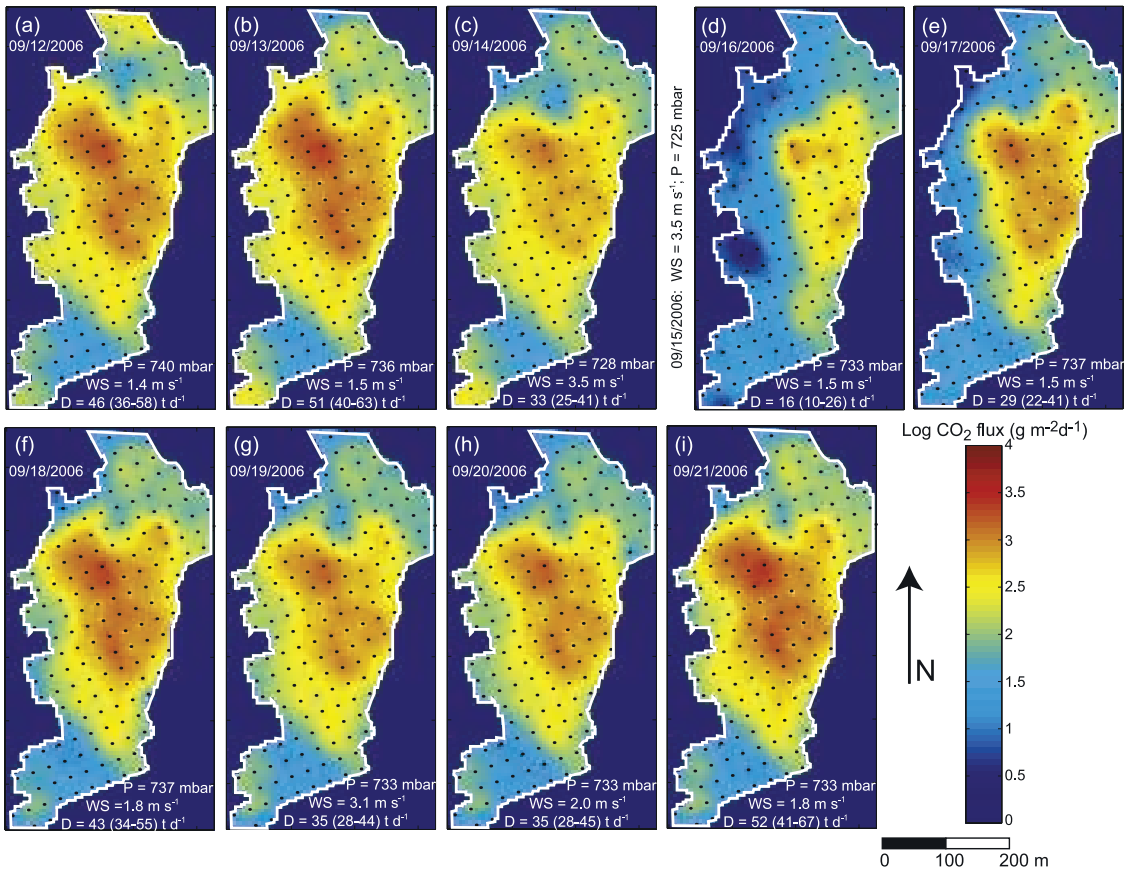

Figure 2. (a–i) Time series of F_{CO2} maps. Black dots are measurement locations. D, WS, and P denote, respectively, CO_2 discharge, average daily wind speed, and average daily atmospheric pressure. Lower and upper 95% bounds on discharge are in parentheses.

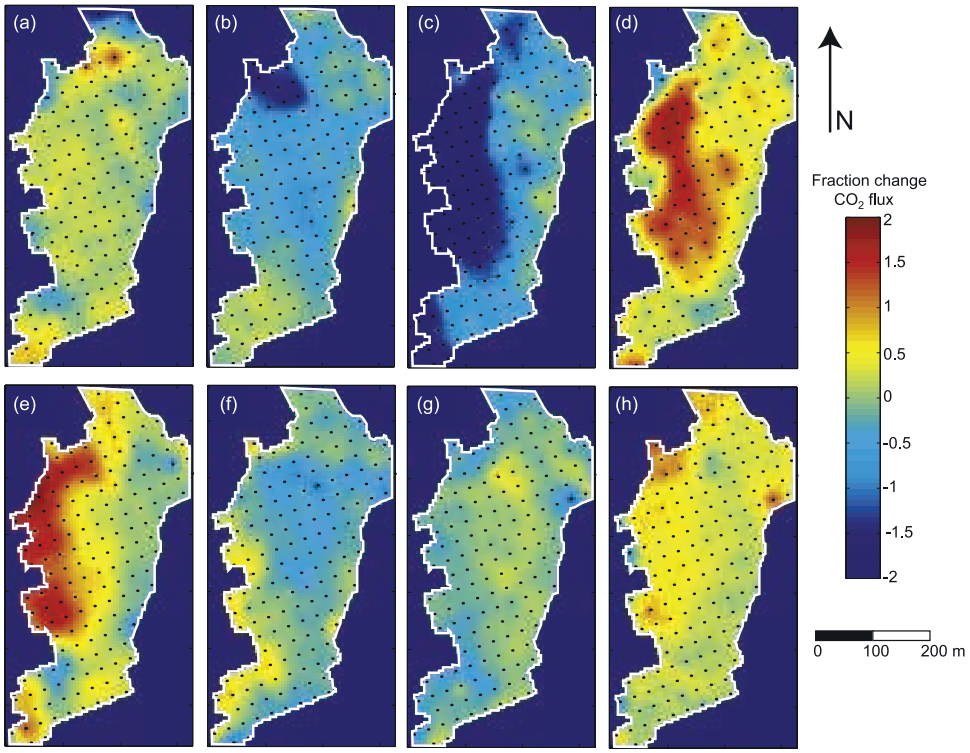

Figure 3. Maps of the fraction change F_{CO2} between (a) 09/12/2006 and 09/13/2006, (b) 09/13/2006 and 09/14/2006, (c) 09/14/2006 and 09/16/2006, (d) 09/16/2006 and 09/17/2006, (e) 09/17/2006 and 09/18/2006, (f) 09/18/2006 and 09/19/2006, (g) 09/19/2006 and 09/20/2006, and (h) 09/20/2006 and 09/21/2006. Fraction change F_{CO2} was calculated by dividing the difference in F_{CO2} between each grid cell for two consecutive days by the mean of the two F_{CO2} values.

to two days time lag (Figure S1). No systematic relationship was observed between CO_2 discharge and average daily atmospheric temperature, atmospheric relative humidity, soil temperature, or soil moisture.

4. Discussion and Conclusions

[11] The spatial distribution of soil CO_2 fluxes we observed at the HLTK is similar to that reported in previous studies [e.g., *Gerlach et al.*, 1998; *Rogie et al.*, 2001]. However, the average estimated CO_2 discharge from the tree kill area was $\sim$250 t d^{-1} (n = 4; range = 130 to 350 t d^{-1}) for 1995 to 1997 [*Gerlach et al.*, 1998] and 93 t d^{-1} (n = 24; range = 45 to 133 t d^{-1}) for 1997 to 2000 [*Rogie et al.*, 2001], whereas the average discharge for the present study was 38 t d^{-1}. If our soil CO_2 flux measurements are representative of the present-day variability of fluxes from the HLTK, then CO_2 emissions have declined markedly. Tracking the long-term rate of decline in CO_2 emissions may help to define the timescale of response to magmatic/fluid intrusion.

[12] The positive correlation observed between CO_2 discharge and average daily atmospheric pressure is the opposite relationship to that expected if barometric pumping were important [e.g., *Nilson et al.*, 1991; *Massmann and Farrier*, 1992]. Thus, it is unlikely that atmospheric pressure exerted a strong influence on average daily CO_2 emissions over the study period, in contrast to that observed by *Rogie et al.* [2001] for soil CO_2 flux on semi-diurnal to diurnal time scales. The negative correlation observed between CO_2 discharge and average daily wind speed suggests that wind acted in some way to suppress CO_2 flow from the soil, with the strongest effect at about one day time lag. Previous studies have documented large-scale wind-driven airflow through unsaturated volcanic rocks [e.g., *Woodcock*, 1987; *Weeks*, 1991]. Soils at the HLTK are largely barren of vegetation, 1 to 3 m thick, and composed of 0.1 to 0.4 m of pumice overlying coarse sand with cobbles to boulders and low organic carbon [*McGee and Gerlach*, 1998; *Evans et al.*, 2001]. Horseshoe Lake is perched, while the water table here is located at $\sim$40 m depth (HSL-1 well) [*Farrar et al.*, 1998], thus potentially allowing for wind-driven airflow through highly porous and permeable material to 10's of meters depth. Also, *Sorey et al.* [1998] measured CO_2 concentrations and $\delta^{13}C$ isotopic compositions of soil gases and showed that while most soil gases were substantially diluted by air, the $\delta^{13}C$ compositions of CO_2 showed significantly less isotopic fractionation of the deep source (magmatic) CO_2 than expected to be associated with purely diffusive transport (W. C. Evans, U.S. Geological Survey, personal communication, 2006). These observations support advective mixing of air with magmatic CO_2 at depth.

[13] Two primary effects of wind on F_{CO2} at the HLTK are considered: a change in CO_2 storage within the shallow vadose zone and a change in the CO_2 source up-flow to the shallow vadose zone. Wind could cause a change in CO_2 storage in the vadose zone, whereby strong winds blowing from the west could drive airflow through the vadose zone, preferentially flushing CO_2 from the soil at relatively high elevations on the western boundary of the study area. Wind-driven flushing of the soils would result in a transient pulse of elevated F_{CO2} above mean values as CO_2 was advectively driven from the soil to the atmosphere. If elevated wind speeds continued after the CO_2 was flushed from the soil, F_{CO2} would return to mean values reflecting the source flux into the vadose zone. Following a decrease in wind speed, we would expect a decline in F_{CO2} below mean values as CO_2 restored concentrations in the vadose zone, assuming the source flux into the bottom of the vadose zone is constant with time. Once vadose zone CO_2 concentrations built up again to equilibrium values, F_{CO2} would return to mean values. Although the flushing mechanism is perhaps the most simple to invoke, we did not observe a period of elevated soil CO_2 discharge during the period of elevated wind speeds, followed by a decline below the mean value with a decline in wind speed. Rather, we documented a decline in CO_2 discharge from the beginning of the windy period (09/14/2006) to its cessation (09/16/2006), followed by a recovery (partially interrupted on 09/19/2006) over the following days. Thus, it is unlikely that wind-driven flushing of CO_2 from the vadose zone accounts for the observed changes in CO_2 emissions at the HLTK. Winds could also cause a change in CO_2 storage by driving lateral airflow through the vadose zone and diverting the CO_2 plume in the direction of prevailing winds. If this occurred, we would expect an eastward-propagating zone of elevated F_{CO2} above mean values as the CO_2 plume was diverted in this direction. Since we did not observe a period of elevated F_{CO2} during the period of high wind speed, rather only a decrease in F_{CO2}, lateral diversion of the CO_2 plume may not account for all aspects of observed changes in CO_2 emissions at the HLTK.

[14] Alternatively, a change (i.e., suppression) in source CO_2 flow at depth within the vadose zone may explain observed changes in CO_2 emissions. This could occur by dynamic coupling of source CO_2 flow to meteorological processes. For example, flow properties of the CO_2 source plume beneath the study area could be altered by lateral atmospheric airflow through the subsurface driven by strong westerly winds. Airflow through the subsurface could change pressure gradients within the vadose zone in a way that retards vertical gas flow to the surface and causes a decrease in surface CO_2 emissions. The observed eastward propagation of this effect over time may be due to westerly winds and/or may reflect a topographic dependence to the coupling. Once subsurface pressures re-equilibrate with the atmosphere and/or airflow through the subsurface ceases, CO_2 emissions would return to mean values.

[15] In summary, we observed large, previously undocumented, spatio-temporal variations in F_{CO2} over multiple days associated with a weather front. These changes may be due to dynamic coupling between the flow of source CO_2 at depth within the vadose zone and wind. However, wind direction, variations in F_{CO2}, and topography were spatially coincident, making it difficult to determine the relative effects of topography and wind direction on F_{CO2}. The spatio-temporal changes in F_{CO2} highlight the strong influence of relatively infrequent weather fronts with strong winds on volcanic gas flow in the near-surface environment, and should be taken into account before attributing changes in gas discharge to deep (e.g., volcanic or seismotectonic) processes. Also, comparative measurements made by different researchers will seem discordant unless performed

together in space and time. Furthermore, the potential effects of topography, wind direction, and wind speed should be considered prior to the placement of continuous monitoring devices within a volcanic area to minimize the influence of background meteorological processes on measured fluxes. Finally, potential dynamic coupling of relatively low-frequency weather fronts with variations in deep source gas flow should be characterized in the field and incorporated into models of gas flow and transport to better understand the role of background processes in spatio-temporal variations of volcanic gas fluxes.

[16] **Acknowledgments.** This work was supported by Zero Emissions Research and Technology (ZERT) and the Ministry of Economy, Trade and Industry (METI) of Japan, through the Lawrence Berkeley National Laboratory Sponsored Project Office contract LB06002281. We thank M. L. Fischer for assistance in the field and G. Chiodini, W. Evans, C. M. Oldenburg, and K. Pruess for helpful review.

References

Bergfeld, D., F. Goff, and C. J. Janik (2001), Elevated carbon dioxide flux at the Dixie Valley geothermal field, Nevada: Relations between surface phenomena and the geothermal reservoir, *Chem. Geol.*, *177*, 43–66.

Cardellini, C., G. Chiodini, and F. Frondini (2003), Application of stochastic simulation to CO_2 flux from soil: Mapping and quantification of gas release, *J. Geophys. Res.*, *108*(B9), 2425, doi:10.1029/2002JB002165.

Chiodini, G., G. R. Cioni, M. Guidi, B. Raco, and L. Marini (1998), Soil CO_2 flux measurements in volcanic and geothermal areas, *Appl. Geochem.*, *13*, 543–552.

Deutsch, C. V. and A. G. Journel (1998), *GSLIB: Geostatistical Software Library and User's Guide*, Oxford Univ. Press, New York.

Evans, W. C., M. L. Sorey, B. M. Kennedy, D. A. Stonestrom, J. D. Rogie, and D. L. Shuster (2001), High CO_2 emissions through porous media: Transport mechanisms and implications for flux measurement and fractionation, *Chem. Geol.*, *177*, 15–29.

Farrar, C. D., M. L. Sorey, W. C. Evans, J. F. Howle, B. D. Kerr, B. M. Kennedy, Y. King, and J. R. Southon (1995), Forest-killing diffuse CO_2 emission at Mammoth Mountain as a sign of magmatic unrest, *Nature*, *376*, 675–678.

Farrar, C. D., J. M. Neil, and J. F. Howle (1998), Magmatic carbon dioxide emissions at Mammoth Mountain, California, *U.S. Geol. Surv. Water Resour. Invest. Rep.*, *98-4217*, 34 pp.

Gerlach, T. M., M. P. Doukas, K. A. McGee, and R. Kessler (1998), Three-year decline of magmatic CO_2 emissions from soils of a Mammoth Mountain tree kill: Horseshoe Lake, CA, 1995–1997, *Geophys. Res. Lett.*, *25*, 1947–1950.

Gerlach, T., M. Doukas, K. McGee, and R. Kessler (2001), Soil efflux and total emission rates of magmatic CO_2 at the Horseshoe Lake tree kill, Mammoth Mountain, California, *Chem. Geol.*, *177*, 101–116.

Giammanco, S., S. Gurrieri, and M. Valenza (1997), Soil CO_2 degassing along tectonic structures on Mount Etna (Sicily): The Pernicana fault, *Appl. Geochem.*, *12*, 429–436.

Hill, D. P. (1996), Earthquakes and carbon dioxide beneath Mammoth Mountain, California, *Seismol. Res. Lett.*, *67*, 8–15.

Hill, D. P., and S. G. Prejean (2005), Volcanic unrest beneath Mammoth Mountain, California, *J. Volcanol. Geotherm. Res.*, *146*, 257–283.

Koepenick, K., S. Brantley, J. Thompson, G. Rowe, A. Nyblade, and C. Moshy (1996), Volatile emissions from the crater and flank of Oldoinyo Lengai volcano, Tanzania, *J. Geophys. Res.*, *101*, 13,819–13,830.

Lewicki, J. L., C. Connor, K. St-Amand, J. Stix, and W. Spinner (2003), Self-potential, soil CO_2 flux, and temperature on Masaya volcano, Nicaragua, *Geophys. Res. Lett.*, *30*(15), 1817, doi:10.1029/2003GL017731.

Lewicki, J. L., D. Bergfeld, C. Cardellini, G. Chiodini, D. Granieri, N. Varley, and C. Werner (2005), Comparative soil CO_2 flux measurements and geostatistical estimation methods on Masaya volcano, Nicaragua, *Bull. Volcanol.*, *68*, 76–90.

Massmann, J., and D. F. Farrier (1992), Effects of atmospheric pressures on gas transport in the vadose zone, *Water Resour. Res.*, *28*, 777–791.

McGee, K. A., and T. M. Gerlach (1998), Annual cycle of magmatic CO_2 in a tree-kill soil at Mammoth Mountain, California: Implications for soil acidification, *Geology*, *26*, 463–466.

McGee, K. A., T. M. Gerlach, R. Kessler, and M. P. Doukas (2000), Geochemical evidence for a magmatic CO_2 degassing event at Mammoth Mountain, California, September–December 1997, *J. Geophys. Res.*, *105*, 8447–8456.

Nilson, R. H., E. W. Peterson, K. H. Lie, N. R. Burkhard, and J. R. Hearst (1991), Atmospheric pumping: A mechanism causing vertical transport of contaminated gases through fractured permeable media, *J. Geophys. Res.*, *96*, 21,933–21,948.

Rogie, J. D., D. M. Kerrick, M. L. Sorey, G. Chiodini, and D. L. Galloway (2001), Dynamics of carbon dioxide emission at Mammoth Mountain, California, *Earth Planet. Sci. Lett.*, *188*, 535–541.

Salazar, J. M., P. A. Hernández, N. M. Pérez, G. Melían, J. Alvarez, F. Segura, and K. Notsu (2001), Diffuse emission of carbon dioxide from Cerro Negro volcano, Nicaragua, Central America, *Geophys. Res. Lett.*, *28*, 4275–4278.

Sorey, M. L., W. C. Evans, B. M. Kennedy, C. D. Farrar, L. J. Hainsworth, and B. Hausback (1998), Carbon dioxide and helium emissions from a reservoir of magmatic gas beneath Mammoth Mountain, California, *J. Geophys. Res.*, *103*, 15,303–15,323.

Weeks, E. P. (1991), Does the wind blow through Yucca Mountain?, in *Proceedings of Workshop V: Flow and Transport Through Unsaturated Fractured Rock Related to High-Level Waste Disposal*, edited by D. D. Evans and T. J. Nicholson, pp. 45–53, U.S. Nucl. Regul. Comm., Rockville, Md.

Werner, C. A., S. L. Brantley, and K. Boomer (2000), CO_2 emissions related to the Yellowstone volcanic system: 2. Statistical sampling, total degassing, and transport mechanisms, *J. Geophys. Res.*, *105*, 10,831–10,846.

Woodcock, A. H. (1987), Mountain breathing revisited—The hyperventilation of a volcano cinder cone, *Bull. Am. Meteorol. Soc.*, *68*, 125–130.

R. Aoyagi and K. Yamamoto, Mizuho Information and Research Institute, 3-1 Kanda-Nishikicho, Chiyoda-ku, Tokyo 101-0054, Japan.

S. M. Benson and J. L. Lewicki, Earth Sciences Division, Lawrence Berkeley National Laboratory, 1 Cyclotron Rd., MS 90-1116, Berkeley, CA 94720, USA. (jllewicki@lbl.gov)

G. E. Hilley, Department of Geological and Environmental Sciences, Stanford University, 450 Serra Mall, Braun Hall, Building 320, Stanford, CA 94305-2115, USA.

T. Tosha, Institute of Geo-Resources and Environment, National Institute of Advanced Industrial Science and Technology, 16-1 Onogawa, Tsukuba, 305-8569, Japan.